Analyst

PAPER

Binding assay for low molecular weight analytes based on reflectometry of absorbing molecules in porous substrates†

Milena Stephan,[a] Corinna Kramer,[b] Claudia Steinem[b] and Andreas Janshoff*[a]

Small molecule sensing is of great importance in pharmaceutical research. While there exist well established screening methods such as EMSA (electrophoretic motility shift assay) or biointeraction chromatography to report on successful binding interactions, there are only a few techniques that allow studying and quantifying the interaction of low molecular weight analytes with a binding partner directly. We report on a binding assay for small molecules based on the reflectivity change of a porous transparent film upon immobilisation of an absorbing substance on the pore walls. The porous matrix acts as a thin optical transparent film to produce interference fringes and accumulates molecules at the inner wall to amplify the sensor response. The benefits and limits of the assay are demonstrated by investigating the binding of biotin labelled with an atto dye to avidin physisorbed within an anodic aluminium oxide membrane.

1. Introduction

Protein interactions with small molecules ($M \leq 500$ Da) play an important role in regulatory biological processes, making small molecules potential candidates for future drugs. The action of the most prospective small molecule drugs is based on their ability to form stable complexes with therapeutic targets. Therefore, characterizing the binding kinetics of small molecule–protein complexes is important in pharmaceutical research.[1] However, quantifying the affinity of the respective binding partners is rather challenging due to the intrinsically low concentration at which the complexes are formed.

Standard kinetic affinity methods may be categorized according to the phase state of the binding partners as heterogeneous or homogeneous. In heterogeneous measurements, one of the binding partners is coupled to a sensor surface, whereas homogeneous methods do not require the immobilisation of any of the binding partners for affinity measurements and are, in general, preferred over heterogeneous methods in protein-small molecule studies.

Perhaps the most prominent technique for homogeneous small molecule interaction studies is the electrophoretic mobility shift assay (EMSA).[2] In EMSA the analyte is incubated with a fixed concentration of a radio-labelled probe and varying amounts of protein. The solutions are run on a native polyacrylamide gel to separate the bound from the free analyte.[2] While EMSA is a very sensitive technique, the probes also have several disadvantages, including safety and environmental problems associated with their radioactivity.

Homogeneous methods generally do not allow the direct observation of binding events. Something that is more easily accomplished with heterogeneous affinity measurements is fluorescence resonance energy transfer (FRET). FRET exploits the energy transfer between two chromophores for sensing purposes. Binding reactions may be sensed with FRET by coupling one interacting agent with a 'donor' and its complementary binding partner with an 'acceptor', whose absorption spectrum overlaps with the donor's emission spectrum.[3] However, using FRET for small molecule sensing can be problematic, since the required labels are often quite large in comparison to the molecules to be investigated and could interfere with the binding activity of both partners.[3]

Most heterogeneous label-free methods such as SPR require the immobilisation of the small interaction partner on the surface of a sensor for sensitive detection since it is easier to monitor the adsorption of the larger binding partner if the detection principle relies on a change in refractive index, for instance. The optical or acoustic signal as a function of the compound concentration can be analysed to obtain both kinetic rates and thermodynamic binding constants. Coupling of a small molecule to a sensor surface, however, may influence its binding ability due to steric reasons.[1] Various workarounds to increase sensing sensitivity have been devised also with a focus on surface plasmon resonance (SPR) spectroscopy. Murthy *et al.* used a strategy to enlarge the detectable mass by adding micelles[4] that display the epitopes of interest to the sensor surface. Alternatively, surface-enhanced fluorescence spectroscopy can be used to boost the detection level

[a]Department of Physical Chemistry, Georg-August University, Göttingen, Germany. E-mail: ajansho@gwdg.de

[b]Department of Organic and Biomolecular Chemistry, Georg-August University, Göttingen, Germany

† Electronic supplementary information (ESI) available. See DOI: 10.1039/c4an00009a

substantially.[5] Usually, however, competition experiments readily circumvent the problem of detection sensitivity due to the small molecular mass of the analyte. In competition experiments the analyte of interest competes with a larger and thus detectable analyte for the immobilised ligand. Moreover, there have been efforts to overcome the problem of small molecule detection by improving the sensitivity of biosensors in general.[6–11] In 2010, Guo *et al.* reported the development of a photonic crystal biosensor for real-time biomolecular binding detection.[12] They used a one-dimensional photonic crystal structure in a total-internal-reflection geometry, creating a sensor that functions as a Fabry–Perot resonator. Using their sensor assembly, they were able to detect the binding of D-biotin ($M = 244$ Da) to streptavidin covalently attached to a surface at D-biotin concentrations as small as 1 μM, but were not able to determine interaction kinetics with their method.[12] Prior to this work, Piehler *et al.* used reflectometric interference spectroscopy (RIfS) to investigate the binding of biotin to a polymerised streptavidin network. RIfS allows determination of the optical thickness (refractive index × physical thickness) of a transparent film deposited on a reflective surface by recording the reflectivity spectrum of the sample. When the sample is irradiated with white light at the right angle, an interference pattern will arise in the reflectivity spectrum originating from the superposition of partial light-beams reflected at the different interfaces of the substrate. The modulation of the interference pattern depends on the path length the light travels inside the transparent film, in other words its optical thickness. Piehler *et al.* were able to measure kinetic curves with their system, but the curves displayed a very large drift, affecting the accuracy of the measurement requiring polymerisation of one binding partner.[13]

Here, we demonstrate a new binding assay for low molecular weight analytes, whose sensing principle is based on the change in reflectivity of a thin porous film upon immobilisation of an absorbing substance. The accumulation of an absorbing agent on the walls of a porous transparent film leads to a detectable change of its extinction coefficient. To our knowledge, this concept has not been used for biomolecular interaction studies before. The potential of the method will be demonstrated by applying the assay to quantify the binding of Atto488-Biotin to avidin physisorbed on anodic aluminium oxide (AAO) substrates.

The association of avidin with biotin is among the strongest known non-covalent protein ligand interactions. The equilibrium dissociation constant K_D of the biotin–avidin complex was found to be 1×10^{-15} M in solution.[14,15] The high affinity of avidin for biotin has led to their use as capture elements in a multitude of biotechnological applications and gave rise to many commercial products.[16] Proteins and peptides, nucleic acids and aptamers have been modified with biotin and immobilised to an avidin surface for use in biological sensing and immunoassays.[17,18] While there are many studies which characterized the binding of avidin to biotin, there were not many successful attempts to try the reverse.[16]

2. Experimental

2.1. Materials

Common chemicals as well as avidin from egg white and Atto488-Biotin were acquired from Sigma Aldrich (Deisenhofen,

Germany). Aluminium with 99.999% purity was purchased from GoodFellow (Coraopolis, Pennsylvania, USA).

2.2. Preparation of Anodic Aluminium Oxide (AAO) membranes

2.2.1. Aluminium metal preparation and electrochemical polishing. Aluminium was annealed at 500 °C overnight to increase the self-organisation of the AAOs to be fabricated. The surface of the substrates was polished using a solution made from concentrated acids ($H_2O/H_3PO_4/H_2SO_4$, 1/1/1). The aluminium plates were warmed to 70 °C, and a constant voltage of 25 V was applied. The electrochemical dissolution of aluminium was continued until the surface became reflective (usually 3–5 min). The process was repeated until the surface was as close to mirror-like as possible, but was done at least 3 times for aluminium supports meant for AAO growth.

2.2.2. AAO membrane growth. The electrochemically polished aluminium plates were placed in an anodization chamber, filled with 0.3 M oxalic acid and cooled under stirring to 1.0 °C. The first anodisation step was carried out at 40 V for 3 h to pre-texture the surface. The oxide layer was dissolved using 5 vol% H_3PO_4 solution over 2–3 h. Anodisation was repeated under the same conditions for 75 min, resulting in 3 μm thick porous membranes. AAOs produced in 0.3 M oxalic acid at 40 V provide an interpore distance of 100 nm and a diameter of 25 nm. The pores were widened to diameters of 60 nm through slow dissolution of the pore material in 5 vol% of H_3PO_4 for 50 min. Functionalisation of the substrate was not necessary. Prior to measurement, the AAO chip was treated with oxygen plasma for 1 min.

2.3. Performing small molecule binding experiments

2.3.1. Set-up. The binding studies were carried out with a home-made RIfS set-up. This type of instrumental assembly has been described in the literature previously.[19,20] A tungsten halogen lamp (LS-1, Ocean Optics, Dunedin, Florida, USA) is used as the light source, from which radiation is coupled into a y-shaped optical fibre (also purchased from Ocean Optics), and guided to a measurement chamber holding a transducer chip, which is irradiated from the top perpendicular to the surface (Fig. 1). The optical fibre consists of six illuminating fibres placed concentrically around one collecting fibre, resulting in a sensing area of 1 mm². The reflected light is gathered by the collecting optical fibre and guided to a spectrometer (Nanocalc-2000-UV/VIS, Ocean Optics).

The measurement chamber was built to allow the exchange of fluids during experiments. For this purpose, a flow channel was milled ($3 \times 10 \times 1$ mm³; volume 30 μl) into an acrylic glass cover. A continuous flow was generated *via* a peristaltic pump (Perimax, Spetec, Erding, Germany). The flow rate was usually set to 1.2 ml min⁻¹.

2.3.2. Adsorption of avidin within AAO membranes. A chip was placed in the measurement chamber of the RIfS set-up and a baseline was recorded in buffer (20 mM HEPES, 100 mM Na_2SO_4, pH = 7.0). After approximately 5 min, a 0.1 mg ml⁻¹ solution of avidin was added and allowed to circulate until the
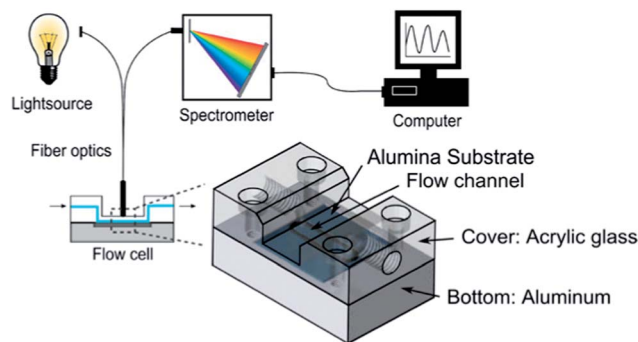
Fig. 1 Schematic drawing of the RIfS setup: light from a tungsten halogen lamp is coupled into a y-shaped optical fibre. The radiation is guided to a flow cell containing the sample. The light reflected by the sample is collected again by the fibre and guided to the spectrometer.
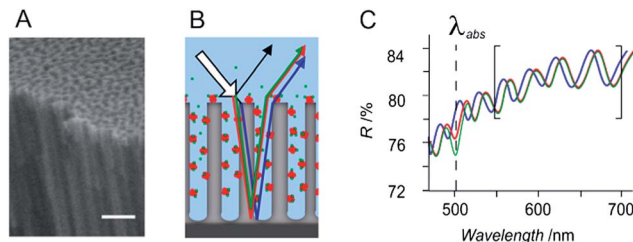

Fig. 2 (A) SEM image of the AAO chip (scale bar: 500 nm). (B) Scheme of the sensing concept. Avidin (red dots) adsorbs on the pore walls of the AAO chip and causes a red shift of the interference spectrum as shown in (C) (blue and red curves). When the dye-labelled biotin (green dots leading to the green beam) binds to the immobilised avidin, the reflectivity of the system is attenuated at the absorption maximum of the Atto dye, which is shown as a drop in the spectrum in (C) (the green curve).

adsorption reaction of avidin to the pore walls of the substrate reached equilibrium (Fig. 3). Buffer was flown through the system until the measured signal stabilized again and the RIfS measurement was terminated.

2.3.3. Monitoring of biotin–avidin interaction. The evaluation software was set to track the reflectivity values of 501 nm radiation (the absorption maximum of Atto488-Biotin). A baseline was recorded 10 min before Atto488-Biotin was added in increasing concentrations (0.5 nM–15 nM) and the system was left to equilibrate after each analyte addition (Fig. 4A). Eventually, the system was rinsed with buffer for 30 min. To determine the equilibrium dissociation constant, measurements were done in triplicate.

2.4. Data processing

2.4.1. Spectrum analysis. All reflectivity spectra recorded during avidin immobilisation and biotin binding were evaluated with RIfS software to track the changes in optical thickness. Additionally, the reflectivity changes for 501 nm radiation, the absorption maximum of the employed fluorescent dye, were read-out. The RIfS evaluation was executed using wavelengths ranging from 550 nm to 700 nm, in order to avoid the analysis being compromised by the absorption effects of the atto dye. A typical reflectivity spectrum is shown in Fig. 2C.

2.4.2. Influence of light-absorbing molecules on reflectivity. Filling the pores with an absorbing medium such as a liquid with dissolved dyes changes the reflectivity of the effective medium comprising the porous matrix (alumina oxide) and the liquid in the pores. It is, however, not possible to detect small amounts of absorbing molecules dissolved in buffer (µM–nM regime) as detailed below. Therefore, adding a solution with dissolved dyes to the porous alumina oxide below 1 mM remains almost invisible to the reflectometric sensor. Only molecules accumulating at the pore walls change the reflectivity of the thin film significantly enough to be detected by a change in reflectivity. The Fresnel coefficients for normal incidence are

$$r_{12} = \frac{n_1 - n_2}{n_1 + n_2}, \tag{1}$$

$$t_{12} = \frac{2n_1}{n_1 + n_2},$$

where n_1 indicates the refractive index of the ambient medium (water) and n_2 is the refractive index of the AAO membrane. n_2 becomes a complex quantity $n_2 = n_{\text{eff}} - \mathrm{i}k_{\text{eff}}$, if an absorbing substance is present in the porous film. n_{eff} and k_{eff} may be calculated according to an effective medium model published by Garahan *et al.*[21] The model predicts the optical properties of nanoporous thin films with horizontally aligned cylindrical nanopores with a specified diameter and porosity.[21]

$$n_{\text{eff}}^2 = \frac{1}{2}\left(A + \sqrt{A^2 + B^2}\right), \tag{2}$$

$$k_{\text{eff}}^2 = \frac{1}{2}\left(-A + \sqrt{A^2 + B^2}\right), \tag{}$$

with

$$A = f(n_{\text{d}}^2 - k_{\text{d}}^2) + (1 - f)(n_{\text{m}}^2 - k_{\text{m}}^2) \tag{3}$$

and

$$B = 2n_{\text{d}}k_{\text{d}}f + 2n_{\text{m}}k_{\text{m}}(1 - f) \tag{4}$$

f denotes the filling factor of domains (pores) present in the substrate, n_{m} and k_{m} are the real and imaginary parts of the refractive index of the substrate material, while n_{d} and k_{d} are the real and imaginary parts of the refractive index of the material forming the domains, respectively. Having calculated the refractive index of the porous layer and the Fresnel coefficients of the system, its reflectivity R may be calculated by

$$R = \left(\frac{r_{12} + t_{12}t_{21}r_{23}\mathrm{e}^{-2\mathrm{i}\delta}}{1 - r_{21}r_{23}\mathrm{e}^{-2\mathrm{i}\delta}}\right)^2, \tag{5}$$

with the phase difference δ

$$\delta = \frac{2\pi}{\lambda}dn_2 \tag{6}$$

between the light-beam reflected on the surface of the substrate and the light-beam refracted into the AAO film. $r_{12}, r_{21}, r_{23}, t_{12}$, and

t_{21} are the typical Fresnel coefficients (*t*: transmission, *r*: reflection) between the media numbered in the subscripts (1: aqueous solution, 2: AAO membrane, 3: alumina substrate).[22]

We found that for a dye such as Atto488 with an extinction coefficient of $8.7 \times 10^4 \text{ M}^{-1} \text{ cm}^{-1}$, and a thickness of alumina oxide of 3000 nm, a concentration of >1 mM in a porous layer of the given geometry and material would be necessary to cause an appreciable change in reflectivity that is detectable by our sensor set-up.[22] Note that $\alpha = \frac{4\pi}{\lambda} k_d$, with α being the extinction coefficient ($I = I_0 e^{-\alpha x}$), k_d being the imaginary part of the refractive index and λ being the corresponding wavelength (here 590 nm). In other words, for a signal change as high as the one measured in our experiment, many more molecules would have to be present in each pore than simply those in the filling solution. This leads to the conclusion that we are able to see the reflectivity changes at very low concentrations since the labelled compound accumulates on the pore walls of the AAO film. The finding agrees well with the concept of the experiment, since the pore walls are functionalised with avidin accumulation of labelled biotin and thus absorbing dye molecules is not only wanted but also expected.

2.4.3. Equilibrium dissociation constant. The reaction of Atto488-Biotin binding to avidin can be described as
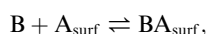
$$B + A_{surf} \rightleftharpoons BA_{surf},$$

where A_{surf} represents the avidin adsorbed in the porous film, B represents the free biotin in solution and BA_{surf} represents the bound complex. The equilibrium dissociation constant K_D can be obtained from the corresponding Langmuir equation[23]

$$\Delta R = \frac{\Delta R_{max} \frac{[B]}{K_D}}{1 + \frac{[B]}{K_D}}, \qquad (7)$$

where ΔR_{max} represents the change in reflectivity obtained when all binding sites on the surface are occupied and ΔR is the steady state signal for any given biotin concentration. K_D is obtained by fitting the parameters K_D and ΔR_{max} of eqn (7) to a graph with ΔR as a function of concentration.

3. Results and discussion

As a sensing principle for this small molecule binding assay we used a variation of reflectometric interference spectroscopy (Fig. 2). If a substance adheres to the walls of a porous AAO film, its refractive index changes. The refractive index may be influenced in two ways. First, the deposition of the material alters the real part of the refractive index of the porous film, increasing its refractive number and thus its optical thickness, which becomes visible as a red-shift of the interference pattern in the reflectivity spectrum of the film (Fig. 2B and C: blue to red curve). This effect was used to measure the adsorption of avidin in the porous layer.

Secondly, another way to influence the refractive index of the porous film is to deposit a small dye-labelled agent on the pore walls. This leads to a change of the extinction coefficient of the porous film. In other words, the reflectivity of the AAO film is attenuated at the absorption maximum of the immobilised

agent, which becomes visible as a drop in the interference pattern of the reflectivity spectrum (Fig. 2B and C: red *vs.* green curve). We utilised this phenomenon to sense the binding of Atto488-Biotin to immobilised avidin as it is more sensitive than monitoring a shift in optical thickness.

Fig. 3 depicts the changes in optical thickness during the deposition of avidin in the porous matrix. The wavelength range used to calculate ΔOT is indicated by the brackets in Fig. 2C. The adsorption of avidin on the pore walls of the AAO film is clearly visible in this graph as an increase in OT of 48 nm immediately after protein addition at point 'a'. Avidin adsorbs on AAOs *via* electrostatic interaction without the help of any surface functionalisation at a pH higher than 3.0.[24] The average surface concentration of avidin $\langle \Gamma(t) \rangle$ as a function of time is at low values of time proportional to the bulk concentration c_b of avidin and the ratio between pore radius R_{pore} and thickness of the AAO membrane d leading to $\langle \Gamma(t) \rangle \propto \frac{R_{pore}}{2d} c_b t$.[24]

Excess protein in solution was removed from the system causing the measured signal to drop by 5 nm (point 'b'). Since avidin was not covalently attached to the pore walls, the continuous flow of liquid through the measurement chamber might affect desorption of avidin molecules, which could be the cause of the constant drift of 1.3 nm h^{-1} seen in the graph. Once the signal stabilized, Atto488-Biotin was added in increasing overall concentration.

Fig. 4A displays the change in reflectivity recorded at 501 nm, close to the adsorption maximum of the attached fluorescent dye Atto488 (as indicated in Fig. 2C). The original data shown in grey were smoothed by averaging over 5 data adjacent points and fit with a monoexponential decay to illustrate the suitability of the Langmuir description. All further data analyses were done with the original data. Once it was confirmed that the reflectivity at the wavelength is stable, the addition of labelled biotin in very low concentrations was started. The binding of Atto488-Biotin to avidin in the AAO membrane is clearly visible in the graph as a decrease of its reflectivity (Fig. 4A). An adsorption isotherm was measured by increasing the concentration of Atto488-Biotin stepwise (concentrations are shown in the graph) and waiting for equilibrium to establish after each successive addition (see ESI, Fig. 1†).
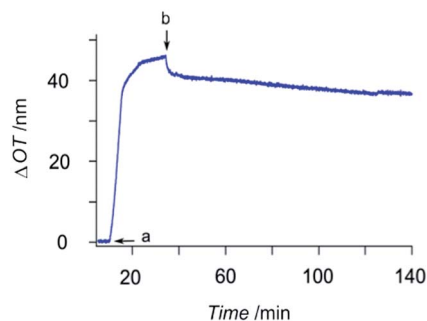

Fig. 3 Change of optical thickness during addition of avidin to an AAO membrane. (a) Avidin addition. The adsorption of avidin on the walls of the porous film leads to an increase of the optical thickness. (b) Rinsing with buffer.
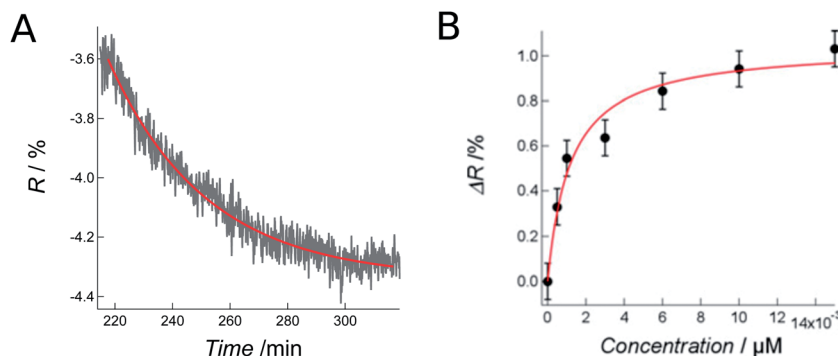
Fig. 4 (A) Change in reflectivity at 501 nm due to adsorption of Atto488-Biotin to an avidin-coated AAO membrane. The original data are shown in grey (smoothed) and the corresponding monoexponential fit in red. Atto488-Biotin was added at an overall concentration of 2 nM. (B) Adsorption isotherm; change in reflectivity as a function of biotin concentration (solid circles). The parameters of the Langmuir equation were fitted to the data (red curve), yielding a K_D value of 1.2 ± 0.3 nM for the avidin–Atto488-Biotin interaction.

In order to prove that the labelled biotin binds to the physisorbed avidin and not the pore wall itself, Atto488-Biotin in a concentration of 100 nM was allowed to circulate over an untreated AAO chip (data not shown). No significant change of its reflectivity was observable upon addition of the labelled compound, indicating that the observations during the actual experiment can safely be attributed to the specific binding of biotin to avidin. Biotin without a label did not produce any noticeable change in reflectivity (ESI, Fig. 2†).

The dissociation constant K_D of the avidin–biotin complex can be determined from adsorption isotherm measurements as shown in graph B of Fig. 4 by fitting the parameters of the Langmuir equation (Experimental section, eqn (7)) to the acquired data. A value of 1.6 ± 0.6 nM was found (the mean value of three independent measurements). This value differs significantly from the dissociation constant of the complex in solution ($K_D = 1 \times 10^{-15}$ M), but is comparable with other surface based techniques, which also reported values in the nanomolar regime.[14–16] There are two possible explanations for the difference of the K_D value determined in solution and the K_D values determined with surface-based sensors.

In 2000, Ben-Tal *et al.* reported that for affinity measurements on surfaces, an entropy loss upon adsorption of one interacting agent on a surface needs to be considered, resulting from the loss of translational degrees of freedom of the said interaction partner that decrease the free energy of binding of the complex by around 1.5 $k_B T$ per degree of freedom.[25] This accounts for higher K_D values determined from surface based techniques compared to those measured in solution. This argument is further strengthened by a study published by Zhao and Reichert that showed the binding kinetics of streptavidin interacting with immobilised biotin differ, if biotin is directly attached to the surface or a spacer is present.[26] Another interesting study was conducted by Sheehan and Whitman in 2005.[27] They calculated the detection limits for nano- and microscale biosensors and were able to show a significant dependence on surface geometry and analyte flow. They deduced that a flat sensor surface is least suitable for low analyte concentration sensing and furthermore that even with ideal geometry, detection schemes based on static or conventional microfluidic flow

systems are unlikely to exceed the femtomolar range. We have to come to the same conclusion as Ben-Tal *et al.* that dissociation constants found for surface-based reactions are usually considerably higher than those measured in solution.

The dynamic range of the sensor scheme lies in between 0.1 and 10 nM for biotin to avidin. The lower concentration regime is limited by the signal to noise ratio that is inherently related to the differences in refractive index and absorbance of the substrate and adsorbent.[22]

4. Conclusion

On the basis of the avidin–biotin model system for high affinity small molecule interaction, we were able to demonstrate the high sensitivity of a new sensing approach which allows for the direct observation and quantification of small molecule binding events. Using fluorescently labelled biotin, we were able to quantify its binding to surface immobilised avidin by sensing the change in reflectivity of the transducer chip at the absorption maximum of the fluorescent dye. Even though, the technique also relies on labelled compounds for detection purposes, which might be considered as a drawback, it offers advantages compared to other small molecule binding assays. The labelling itself is not restricted to rather bulky fluorescent dyes. The only criterion the label would have to meet is that its absorption maximum lies in between the medium UV and the near infrared spectrum to produce an appreciable absorption peak in the reflectivity spectrum. This allows for the use of smaller compounds than the conventional fluorescent dyes. Another advantage compared to assay formats based on fluorescence is that the measurements are not notably affected by photobleaching. Furthermore, employing an anodic alumina oxide membrane as a transducer chip, a well established substrate for biosensing, opens the possibility of various applications for this binding assay, since a library of surface functionalisation is readily available. Yet another advantage of this sensor compared to other techniques based on planar surfaces is that it offers the opportunity to directly observe binding events and to measure equilibrium dissociation constants in the low nanomolar regime with a very simple and inexpensive instrumental

arrangement. In the future, it is conceivable to combine the AAO chip with other more sensitive optical transducers.[28]

Acknowledgements

References

1 J. Bao and S. N. Krylov, Volatile kinetic capillary electrophoresis for studies of protein-small molecule interactions, *Anal. Chem.*, 2012, **84**, 6944–6947.

2 A. E. Dahlberg, C. W. Dingman and A. C. Peacock, Electrophoretic characterization of bacterial polyribosomes in agarose–acrylamide composite gels, *J. Mol. Biol.*, 1969, **41**, 139–147.

3 R. Laine, D. W. Stuckey, H. Manning, S. C. Warren, G. Kennedy, D. Carling, C. Dunsby, A. Sardini and P. M. W. French, Fluorescence lifetime readouts of troponin-c-based calcium fret sensors: a quantitative comparison of cfp and mtfp1 as donor fluorophores, *PLoS One*, 2012, **7**, e49200.

4 B. N. Murthy, N. H. Voelcker and N. Jayaraman, Evaluation of a-ᴅ-mannopyranoside glycolipid micelles–lectin interactions by surface plasmon resonance method, *Glycobiology*, 2006, **16**, 822–832.

5 S. Ekgasit, F. Yu and W. Knoll, Fluorescence intensity in surface-plasmon field-enhanced fluorescence spectroscopy, *Sens. Actuators, B*, 2005, **104**, 822–832.

6 J. N. Anker, W. P. Hall, O. Lyandres, N. C. Shah, J. Zhao and R. P. Van Duyne, Biosensing with plasmonic nanosensors, *Nat. Mater.*, 2008, **7**(6), 442–453, DOI: 10.1038/nmat2162.

7 R. Miller, V. B. Fainerman, A. V. Makievski, J. Krägel, D. O. Grigoriev, V. N. Kazakov and O. V. Sinyachenko, Dynamics of protein and mixed protein/surfactant adsorption layers at the water/fluid interface, *Adv. Colloid Interface Sci.*, 2000, **86**(1–2), 39–82.

8 A. K. Naik, M. S. Hanay, W. K. Hiebert, X. L. Feng and M. L. Roukes, Towards single-molecule nanomechanical mass spectrometry, *Nat. Nanotechnol.*, 2009, **4**(7), 445–450, DOI: 10.1038/nnano.2009.152.

9 V. C. Ozalp, Dual-polarization interferometry for quantification of small molecules using aptamers, *Anal. Bioanal. Chem.*, 2012, **402**(2), 799–804, DOI: 10.1007/s00216-011-5499-9.

10 F. Patolsky, G. Zheng and C. M. Lieber, Nanowire sensors for medicine and the life sciences, *Nanomedicine*, 2006, **1**(1), 51–65, DOI: 10.2217/17435889.1.1.51.

11 H. Habib Qazi, A. B. Bin Mohammad and M. Akram, Recent progress in optical chemical sensors, *Sensors*, 2012, **12**(12), 16522–16556, DOI: 10.3390/s121216522.

12 Y. Guo, J. Y. Ye, C. Divin, B. Huang, T. P. Thomas, J. R. Baker and T. B. Norris, Real-time biomolecular binding detection using a sensitive photonic crystal biosensor, *Anal. Chem.*, 2010, **82**, 5211–5218.

13 J. Piehler, A. Brecht and G. Gauglitz, Affinity detection of low molecular weight analytes, *Anal. Chem.*, 1996, **68**, 139–143.

14 N. M. Green, Avidin and streptavidin, *Methods Enzymol.*, 1990, **184**, 51–67.

15 M. Wilchek and E. A. Bayer, Introduction to avidin–biotin technology, *Methods Enzymol.*, 1990, **184**, 5–13.

16 G. R. Broder, R. T. Ranasinghe, C. Neylon, H. Morgan and P. L. Roach, Kinetics and thermodynamics of biotinylated oligonucleotide probe binding to particle-immobilized avidin and implications for multiplexing applications, *Anal. Chem.*, 2011, **83**, 2005–2011.

17 J. W. Chung, J. M. Park, R. Bernhardt and J. C. Pyun, Immunosensor with a controlled orientation of antibodies by using neutravidin-protein a complex at immunoaffinity layer, *J. Biotechnol.*, 2006, **126**, 325–333.

18 N. Haddour, J. Chauvin, C. Gondran and S. Cosnier, Photoelectrochemical immunosensor for label-free detection and quantification of anti-cholera toxin antibody, *J. Am. Chem. Soc.*, 2006, **128**(30), 9693–9698.

19 G. Gauglitz, A. Brecht, G. Kraus and W. Nahm, Chemical and biochemical sensors based on interferometry at thin (multi-) layers, *Sens. Actuators, B*, 1993, **11**, 21–27.

20 A. Janshoff, K. P. S. Dancil, C. Steinem, D. P. Greiner, V. S. Y. Lin, C. Gurtner, K. Motesharei, M. J. Sailor and M. R. Ghadiri, Macroporous p-type silicon Fabry–Perot layers. fabrication, characterization, and applications in biosensing, *J. Am. Chem. Soc.*, 1998, **46**, 12108–12116.

21 A. Garahan, L. Pilon and J. Yin, Effective optical properties of absorbing nanoporous and nanocomposite thin films, *J. Appl. Phys.*, 2007, **101**, 014320.

22 O. Stenzel, *The Physics of Thin Film Optical Spectra: An Introduction*, Springer Series in Surface Sciences, 2010, pp. 107–110

23 H. J. Butt, K. Graf and M. Kappl, *Physics and Chemistry of Interfaces*, Wiley-VCH Verlag GmbH and Co KGaA, Weinheim, 1st edn, 2003.

24 T. D. Lazzara, I. Mey, C. Steinem and A. Janshoff, Benefits and limitations of porous substrates as biosensors for protein adsorption, *Anal. Chem.*, 2011, **83**, 5624–5630.

25 N. Ben-Tal, B. Honig, C. K. Bagdassarian and A. Ben-Shaul, Association entropy in adsorption processes, *Biophys. J.*, 2000, **79**, 1180–1187.

26 S. Zhao and W. M. Reichert, Influence of biotin lipid surface-density and accessibility of avidin binding to the tip of an optical fiber, *Langmuir*, 1992, **8**, 2785–2791.

27 P. E. Sheehan and L. J. Whitman, Detection limits for nanoscale biosensors, *Nano Lett.*, 2005, **5**, 803–807.

28 M. A. Cooper, Optical biosensors in drug discovery, *Nat. Rev. Drug Discovery*, 2002, **1**(7), 515–528, DOI: 10.1038/nrd838.